Measurement of forward charged hadron flow harmonics in peripheral PbPb collisions at $\sqrt{s_{NN}} = 5.02$ TeV with the LHCb detector

R. Aaij *et al.**
(LHCb Collaboration)

(Received 16 November 2023; accepted 27 March 2024; published 15 May 2024)

Flow harmonic coefficients, v_n, which are the key to studying the hydrodynamics of the quark-gluon plasma (QGP) created in heavy-ion collisions, have been measured in various collision systems and kinematic regions and using various particle species. The study of flow harmonics in a wide pseudorapidity range is particularly valuable to understand the temperature dependence of the shear viscosity to entropy density ratio of the QGP. This paper presents the first LHCb results of the second- and the third-order flow harmonic coefficients of charged hadrons as a function of transverse momentum in the forward region, corresponding to pseudorapidities between 2.0 and 4.9, using the data collected from PbPb collisions in 2018 at a center-of-mass energy of 5.02 TeV. The coefficients measured using the two-particle angular correlation analysis method are smaller than the central-pseudorapidity measurements at ALICE and ATLAS from the same collision system but share similar features.

DOI: 10.1103/PhysRevC.109.054908

I. INTRODUCTION

Quark-gluon plasma (QGP) is a phase of nuclear matter in which partons can move freely, as explained by the asymptotic freedom of quantum chromodynamics (QCD). The QGP medium is formed in an extremely hot and dense environment, such as in high energy collisions of heavy-ions [1–5]. As the heavy ions collide at near the speed of light, a dense QGP medium forms and thermalizes rapidly.

The unbound partons of the QGP move collectively. This collective movement is heavily affected by the initial collision conditions, such as the momentum anisotropy due to the asymmetric collision geometry. These conditions cause spatial anisotropy in the final particle distributions. The study of the spatial anisotropy, commonly known as flow, helps us to understand the evolution and the properties of the QGP, including the thermalization process, initial- and final-state effects, and the transport properties including the ratio of shear viscosity to entropy density. The value of the ratio of shear viscosity to entropy density is found to be small [6], which indicates that the QGP medium behaves like a nearly perfect fluid.

Several theory models predict that the ratio of shear viscosity to entropy density is temperature dependent [7–9]. The study of this temperature dependence requires a wide range of particle flow measurements, covering different collision energies, centralities, transverse momenta, and pseudorapidities, such as those reported by experiments at both the BNL Relativistic Heavy Ion Collider (RHIC) and the CERN Large Hadron Collider (LHC). Measurements to date include pp, dAu, ^{3}HeAu, XeXe, AuAu, and PbPb collision systems [10–15], energies ranging from $\mathcal{O}$(GeV) to $\mathcal{O}$(TeV) [16–18], and the most central events to ultraperipheral collisions [18,19]. Most of these results are presented in the central pseudorapidity region, $|\eta| < 2.5$. Several forward (large $|\eta|$) particle flow studies were reported by PHOBOS using AuAu collisions at the GeV energy scale [20,21] and by ALICE using PbPb and pPb collisions at the TeV energy scale [22–24].

The LHCb experiment can provide unique flow measurements in the forward region, which are important to understand the "cooler" region where freeze-out is dominant [8]. The forward region is dominated by the nonequilibrium hadronic phase and can test the limit of the hydrodynamic and the transport models that describe QGP at microscopic and macroscopic scales, respectively. LHCb measurements also complement other LHC results that are in the central-pseudorapidity regions in the effort to constrain theoretical models and understand the evolution of QGP.

This paper reports the first measurement of the forward flow harmonic coefficient of charged hadrons as a function of transverse momentum at LHCb and at the LHC to enrich the study of flow in the nonequilibrium hadronic phase of the system evolution. The two-dimensional $[C(\Delta\eta, \Delta\phi)]$ and one-dimensional $[C(\Delta\phi)]$ correlation functions are constructed using a two-particle correlation analysis method [12,25,26]. The one-dimensional azimuthal correlation functions are described by a Fourier series, which is used to extract the second- and third-order flow harmonic coefficients, v_2 and v_3. The two-particle correlation analysis method is applied

*Full author list given at the end of the article.

to data in two centrality ranges, 65%–75% and 75%–84%, determined in Ref. [27]. The flow harmonic coefficients are measured as a function of transverse momentum, p_{T}. The results are compared to those from the ALICE and ATLAS experiments at central pseudorapidity in PbPb collisions at 5.02 TeV [18,25] and to simulations based on the multiphase transport model AMPT [28,29].

II. THE LHCb EXPERIMENT

The analysis is based on data collected with the LHCb detector during the lead-lead data-taking period in 2018. The LHC provided PbPb collisions at a nucleon–nucleon center-of-mass energy of $\sqrt{s_{NN}} = 5.02\,\mathrm{TeV}$, corresponding to an integrated luminosity of 214 $\mu\mathrm{b}^{-1}$.

The LHCb detector [30,31] is a single-arm forward spectrometer covering the pseudorapidity range $2 < \eta < 5$, designed for the study of particles containing b or c quarks. The detector includes a high-precision tracking system consisting of a silicon-strip vertex detector (VELO), surrounding the PbPb interaction region [32], a large-area silicon-strip detector located upstream of a dipole magnet with a bending power of about 4 T m, and three stations of silicon-strip detectors and straw drift tubes [33,34] placed downstream of the magnet. The tracking system provides a measurement of the momentum, p, of charged particles with a relative uncertainty that varies from 0.5% at low momentum to 1.0% at 200 GeV/c. The minimum distance of a track to a primary PbPb collision vertex (PV), the impact parameter (IP), is measured with a resolution of $(15 + 29/p_{\mathrm{T}})$ μm, with p_{T} in GeV/c. Photons, electrons and hadrons are identified by a calorimeter system consisting of scintillating-pad and preshower detectors (SPD), an electromagnetic calorimeter, and a hadronic calorimeter. The online event selection is performed by a trigger [35], which consists of a hardware stage, based on information from the calorimeter and muon systems, followed by a software stage, which applies a full event reconstruction.

Simulation samples are required to model the effects of the detector acceptance and the selection requirements. The PbPb events are generated using the EPOS event generator [36] and calibrated with LHC data [37]. Decays of unstable particles are described by EVTGEN [38], in which final-state radiation is generated using PHOTOS [39]. The interaction of the generated particles with the detector, and its response, are implemented using the GEANT4 toolkit [40] as described in Ref. [41].

III. DATA SELECTION

The PbPb events must satisfy at least one of four minimum-bias triggers, all of which place requirements on the number of SPD hits. Two of them impose further requirements based on information from either the hadronic calorimeter or the muon system. Due to hardware limitations, only events with fewer than ten thousand VELO clusters are recorded, which corresponds to centrality greater than 60%.

Events with a PV within $\pm 3\sigma$ of the mean PV z coordinate, where σ is the width of the PV z distribution for the dataset, and a centrality between 65–84% determined by the total calorimeter energy [27] are selected. Centrality ranges below 65% are avoided due to lack of sufficient events. The upper bound of the centrality selection is set to avoid contamination with ultraperipheral events [27]. The data are contaminated with fixed-target PbNe collisions that were running simultaneously with the PbPb collisions. Since the PbNe events have lower center-of-mass energy and lower average multiplicity, the selected PbPb events must have at least 15 tracks in the backward ($\eta < -2$) region and are required to have a minimum total calorimeter energy that depends on the number of VELO clusters.

All tracks selected in this analysis are measured by the VELO, the silicon-strip detectors located upstream and downstream of the magnet, and the straw drift tubes. These tracks have a minimum momentum of 2 GeV/c. The selected tracks must have $p_{\mathrm{T}} > 0.2\,\mathrm{GeV}/c$, $2 < \eta < 4.9$, and a small fit χ^2. Tracks from the decays of heavy-flavor hadrons are suppressed by a requirement on the change in the primary vertex χ^2 when the track is excluded from the vertex fit.

IV. TWO-PARTICLE ANGULAR CORRELATION ANALYSIS

Two-particle correlation analysis is based on the fact that the correlations among the produced particles reflect the correlations between the produced particles and the reaction plane [42], that is the azimuth of the impact parameter. Two tracks from the same event, labeled a and b, are paired to construct the two-dimensional angular distributions, $S(\Delta\eta, \Delta\phi)$, where $\Delta\eta = \eta_a - \eta_b$ and $\Delta\phi = \phi_a - \phi_b$. The transverse momentum of track a is in one of several p_{T} ranges defined within $0.2 < p_{\mathrm{T}a} < 10\,\mathrm{GeV}/c$, but that of track b must be within $0.2 < p_{\mathrm{T}b} < 5\,\mathrm{GeV}/c$ regardless of $p_{\mathrm{T}a}$. The lower bound of $p_{\mathrm{T}b}$ is set according to the tracking performance of the detector [43], while the upper bound is set to reduce jet-like contributions at high p_{T} [25]. Applying the same track requirements, two tracks from different events are also paired to construct the mixed-event angular distributions, $B(\Delta\eta, \Delta\phi)$, which carry any biases from the detector acceptance.

The two-dimensional angular correlation functions, $C(\Delta\eta, \Delta\phi)$, are obtained by correcting the same-event correlations using the mixed-event correlations, such that

$$C(\Delta\eta, \Delta\phi) = \frac{S(\Delta\eta, \Delta\phi)}{B(\Delta\eta, \Delta\phi)}. \tag{1}$$

Figure 1 shows an example of the two-dimensional angular correlation functions for $1 < p_{\mathrm{T}a,b} < 2\,\mathrm{GeV}/c$ and $2 < p_{\mathrm{T}a,b} < 3\,\mathrm{GeV}/c$ and in centrality ranges 65%–75% and 75%–84%. These two $p_{\mathrm{T}a,b}$ ranges are selected to match Ref. [44] for comparisons, but the rest of the analysis shown below used the fixed $p_{\mathrm{T}b}$ range of 0.2–5 GeV/c. A clear near-side peak at $(\Delta\eta, \Delta\phi) = (0, 0)$, which arises from the short-range nonflow contributions [45], such as jets, is observed in both p_{T} ranges and centrality ranges. A dip at the center of the near-side peak is observed in the low p_{T} range in the 65–75% centrality range. This dip is caused by the removal of tracks that share 70% of hits in the track reconstruction [46]. There are ridge structures on the near side ($\Delta\phi \approx 0$) and away side ($\Delta\phi \approx \pi$). The near-side ridges, which are less

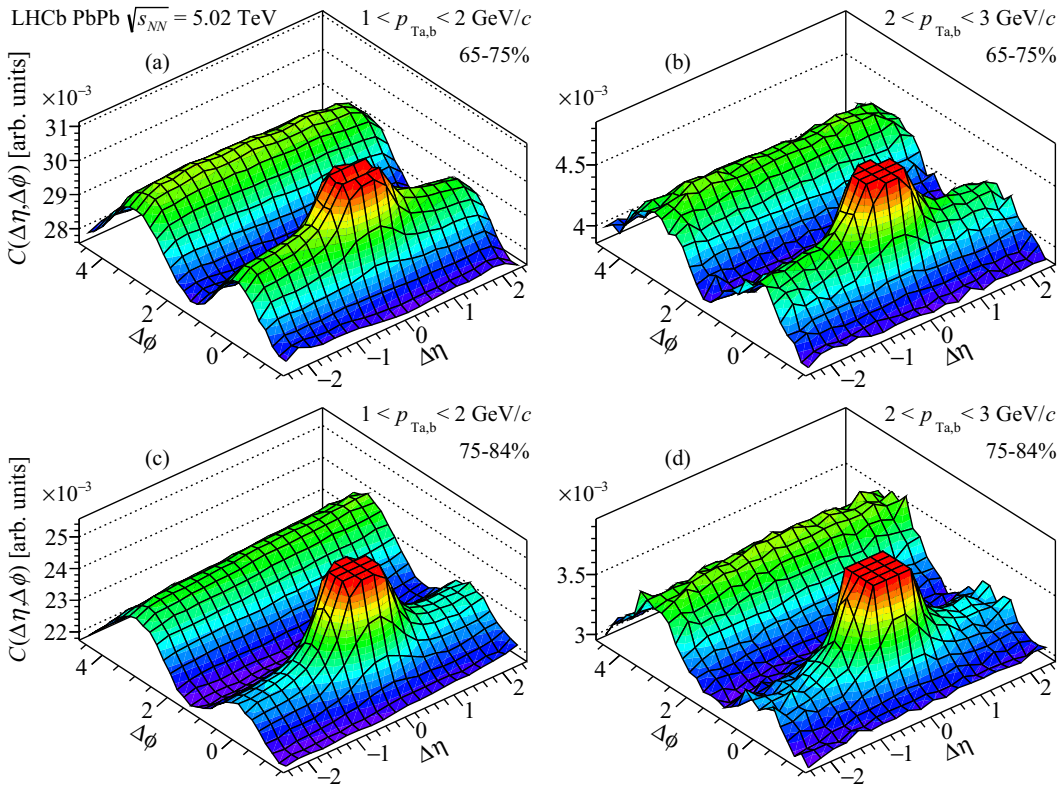

FIG. 1. Angular correlation functions in four example intervals of transverse momentum and centrality. The $\Delta\eta$ range is limited to ± 2.5. The z axis is cropped to visualize the ridge structures.

noticeable than the away-side ridges, are a sign of particle flow [44]. The near-side ridges are more pronounced in Fig. 1 compared to the correlation functions in pPb and Pbp collisions in Ref. [44], indicating stronger flow in PbPb collisions.

One-dimensional azimuthal correlation functions, $C(\Delta\phi)$, are obtained by taking the ratio of the projection of $S(\Delta\eta, \Delta\phi)$ and $B(\Delta\eta, \Delta\phi)$ onto the $\Delta\phi$ axis. The $|\Delta\eta| < 1$ region is removed in the projection to reduce short-range nonflow contributions, such that the azimuthal correlation function is

$$C(\Delta\phi) = \frac{\int_1^{2.9} S(|\Delta\eta|, \Delta\phi) \cdot d(|\Delta\eta|)}{\int_1^{2.9} B(|\Delta\eta|, \Delta\phi) \cdot d(|\Delta\eta|)}. \quad (2)$$

A Fourier series fit to this function is performed including the first three harmonic terms,

$$C(\Delta\phi) = A\left[1 + 2\sum_{n=1}^{3} V_n(\langle p_{\mathrm{T}a}\rangle, \langle p_{\mathrm{T}b}\rangle)\cos(n \cdot \Delta\phi)\right], \quad (3)$$

where $\langle p_{\mathrm{T}a}\rangle$ ($\langle p_{\mathrm{T}b}\rangle$) represents the average $p_{\mathrm{T}a}$ ($p_{\mathrm{T}b}$) for the given $p_{\mathrm{T}a}$ ($p_{\mathrm{T}b}$) range, A and $V_n(\langle p_{\mathrm{T}a}\rangle, \langle p_{\mathrm{T}b}\rangle)$ are parameters that vary freely in the fit. The coefficient $V_n(\langle p_{\mathrm{T}a}\rangle, \langle p_{\mathrm{T}b}\rangle)$ extracted from the fit can be factorized as

$$V_n(\langle p_{\mathrm{T}a}\rangle, \langle p_{\mathrm{T}b}\rangle) = v_n^a(\langle p_{\mathrm{T}a}\rangle) \cdot v_n^b(\langle p_{\mathrm{T}b}\rangle), \quad (4)$$

where $v_n^a(\langle p_{\mathrm{T}a}\rangle)$ ($v_n^b(\langle p_{\mathrm{T}b}\rangle)$) is the n^{th} flow harmonic coefficient of particle a (b) with a transverse momentum in $\langle p_{\mathrm{T}a}\rangle$ ($\langle p_{\mathrm{T}b}\rangle$) [47]. Since the $p_{\mathrm{T}b}$ range is fixed regardless of the $p_{\mathrm{T}a}$ interval, one can first obtain $v_n^b(\langle p_{\mathrm{T}b}\rangle)$ by constructing the azimuthal correlations in Eq. (3) of tracks from the b tracks only. Then, Eq. (4) becomes

$$V_n(\langle p_{\mathrm{T}b}\rangle, \langle p_{\mathrm{T}b}\rangle) = v_n^b(\langle p_{\mathrm{T}b}\rangle) \cdot v_n^b(\langle p_{\mathrm{T}b}\rangle), \quad (5)$$

which implies

$$v_n^b(\langle p_{\mathrm{T}b}\rangle) = \sqrt{V_n(\langle p_{\mathrm{T}b}\rangle, \langle p_{\mathrm{T}b}\rangle)}. \quad (6)$$

The flow harmonic coefficient of particle a, $v_n^a(\langle p_{\mathrm{T}a}\rangle)$, from the track a-b azimuthal correlations is obtained by substituting Eq. (6) into Eq. (4).

However, this factorization in Eqs. (4) and (6) does not apply to the first-order flow harmonic coefficient, as it is strongly affected by the long-range nonflow contributions [45,47]. Therefore, the first-order flow harmonic coefficient, v_1, is not reported. These long-range nonflow contributions may also affect the higher-order flow harmonic coefficients in peripheral events at high p_{T} [25,45]. These effects include the increase and decrease of the even- and odd-order flow harmonic coefficients, respectively, at high p_{T}. Since only $v_n^a(\langle p_{\mathrm{T}a}\rangle)$ results are shown, in the rest of this paper v_n and p_{T} denote v_n^a and $\langle p_{\mathrm{T}a}\rangle$, respectively.

Figure 2 shows examples of the azimuthal correlation functions overlaid with the Fourier series fit results in different p_{T} and centrality ranges. The relative difference in amplitudes between the near- and away-side peaks is enhanced at high p_{T} and in peripheral events. The second- and third-order flow harmonic coefficients, $v_2(p_{\mathrm{T}})$ and $v_3(p_{\mathrm{T}})$, are extracted from the Fourier series fits in different p_{T} and centrality ranges.

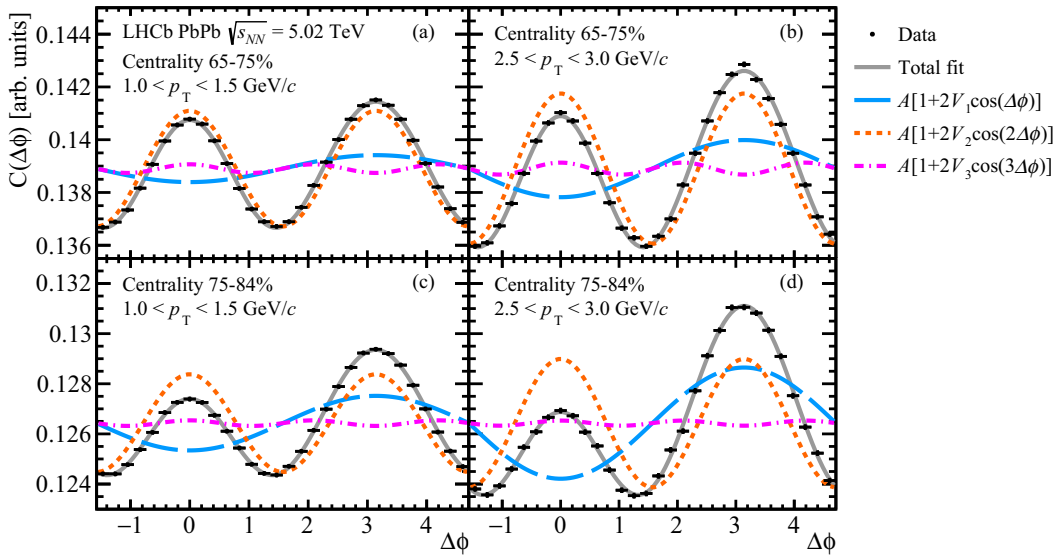

FIG. 2. Azimuthal correlation functions in different transverse momentum and centrality ranges. The Fourier series fit and its three terms are overlaid. Only statistical uncertainties are shown.

V. SYSTEMATIC UNCERTAINTIES

The total systematic uncertainty is obtained from the sum in quadrature of the following six contributions: (a) the primary vertex requirement, (b) the track fit quality requirement, (c) the total calorimeter energy versus VELO multiplicity requirements for PbNe event contamination, (d) Fourier fit fluctuation, (e) fluctuation of the mixed-event correlations, and (f) the unidentified charged hadron efficiency and fake track rate. These systematic uncertainties are estimated by taking the difference of the nominal result and results obtained with alternate requirements as follows.

(a) The primary vertex z requirement is varied between 2 and 4 standard deviations of the width of the distribution.

(b) The track fit χ^2 requirement is tightened and relaxed such that the p_T distribution with the tightened or relaxed requirement is on average 10% different compared to the default requirement.

(c) Besides the minimum total calorimeter energy requirement in the event selection, an additional maximum total calorimeter energy requirement that depends on the number of VELO clusters is applied to remove outlier events with high total calorimeter energy but low multiplicity.

(d) A fourth-order harmonic term is added to the Fourier series fit in Eq. (3).

(e) The analysis is repeated by moving each data point individually in the mixed-event correlations to its upper and lower statistical limits.

(f) The nominal values of the v_n measurements are obtained without correcting for the detector efficiency, $\epsilon(p_T, \eta)$, and the fake track rate, $f(p_T, \eta)$. To estimate the systematic uncertainties due to the detector efficiency and the fake track rate, the analysis is repeated with the detector efficiency and the fake track rate corrections as a track-paired weight, w. The track-paired weight, which is applied when filling two-dimensional angular distributions, is written as

$$w = \frac{1 - f(p_{Ta}, \eta_a)}{\epsilon(p_{Ta}, \eta_a)} \times \frac{1 - f(p_{Tb}, \eta_b)}{\epsilon(p_{Tb}, \eta_b)}. \quad (7)$$

The relative systematic uncertainties due to the above sources are summarized in Table I for three p_T ranges:[1] $0.2 < p_T < 0.4\,\text{GeV}/c$, $0.4 < p_T < 3\,\text{GeV}/c$, and $3 < p_T < 10\,\text{GeV}/c$. The relative uncertainties are larger in

[1]The final results are presented with 12 p_T bins.

TABLE I. Summary of relative systematic uncertainties rounded to the closest 1%.

p_T (GeV/c)	σ_a	σ_b	σ_c	σ_d	σ_e	σ_f
			v_2 in 65–75%			
0.2–0.4	4%	19–22%	<1%	<1%	<1%	6%
0.4–3	<1%	<5%	<1%	<1%	<1%	<5%
3–10	<4%	<5%	<1%	<1%	<1%	<10%
			v_2 in 75–84%			
0.2–0.4	<1%	17–18%	<1%	<1%	<1%	27%
0.4–3	<1%	<3%	<1%	<1%	<1%	<6%
3–10	<1%	<4%	<1%	<1%	<1%	1–17%
			v_3 in 65–75%			
0.2–0.4	14%	23–34%	2%	<1%	5%	64%
0.4–3	<5%	<19%	<2%	<1%	<2%	3–9%
3–10	2–54%	<152%	<9%	<2%	4–22%	7–133%
			v_3 in 75–84%			
0.2–0.4	13%	21–28%	1%	<1%	2%	14%
0.4–3	<9%	<20%	<2%	<1%	1–4%	2–35%
3–10	1–56%	21–142%	1–20%	1–8%	5–31%	18–146%

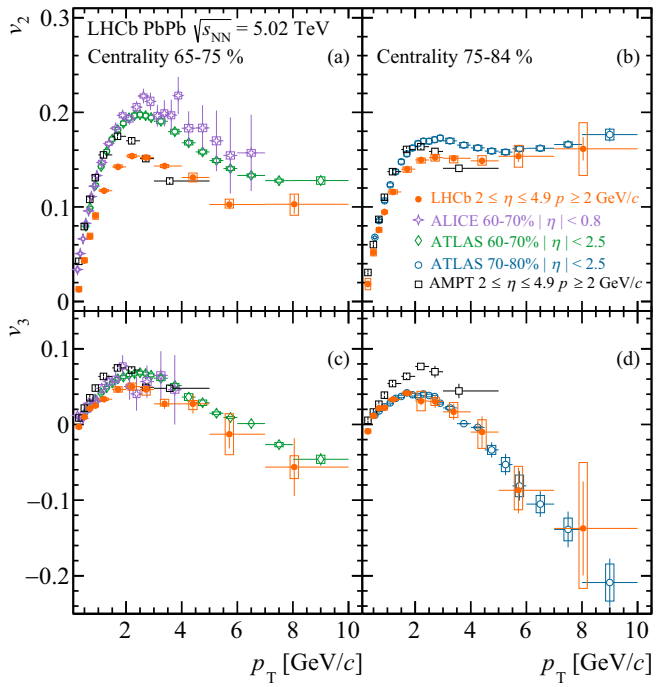

FIG. 3. Second- and third-order flow harmonic coefficients as functions of transverse momentum. The statistical and systematic uncertainties are drawn as error bars and boxes, respectively. Only statistical uncertainties are shown for the AMPT predictions.

$0.2 < p_T < 0.4\,\text{GeV}/c$ and in $3 < p_T < 10\,\text{GeV}/c$, where the nominal v_n is closer to zero or the statistics is low. Furthermore, the relative uncertainties of v_3 are generally larger than those of v_2 since v_3 is closer to zero than v_2. Uncertainty sources (b) track fit quality and (f) hadron efficiency and fake track rate are two major contributors to the systematic uncertainties of v_2 and v_3 in all three p_T ranges. Uncertainty sources (a) primary vertex requirement and (e) fluctuation of mixed-event correlations are subdominant for v_3 in the ranges $0.2 < p_T < 0.4\,\text{GeV}/c$ and $3 < p_T < 10\,\text{GeV}/c$.

VI. RESULTS

Figure 3 shows the measured second- and third-order forward flow harmonic coefficients, v_2 and v_3, as a function of p_T in PbPb collisions at center-of-mass energy of 5.02 TeV. The numerical results are given in the Appendix. These data are compared to ALICE and ATLAS results [18,25] and AMPT simulations [28,29]. The second- and third-order flow harmonic coefficients rise at low p_T and then turn downward after 2.5 GeV/c. Above 5 GeV/c, the v_2 values are consistent as the uncertainties increase at high p_T. Unlike v_2, v_3 continues to decrease at p_T greater than 2.5 GeV/c and goes below zero at p_T greater than 5 GeV/c. The consistent v_2 and continuous falling of v_3 at high p_T hint at factorization breaking due to residual nonflow contributions at high p_T [25,45].

The ALICE and ATLAS results for v_2 and v_3 at central pseudorapidity are also extracted from PbPb collision data at center-of-mass energy of 5.02 TeV in centrality ranges of 60%–70% and 70%–80%. The ALICE and ATLAS results are obtained using the two-particle cumulants and two-particle correlation analysis methods, respectively. These results share similar features, but higher values compared to this paper due to differences in pseudorapidity ranges. This pseudorapidity dependence has also been observed by the PHOBOS [20] and ALICE [22] experiments.

AMPT simulates particle flow with a string melting model that produces a dense system of partonic matter, and includes quark coalescence to improve the modeling of elliptic flow [29]. The AMPT simulations with 68.5-million events overestimate the forward v_2 at $p_T < 2.5\,\text{GeV}/c$, and the forward v_3 at $p_T < 5\,\text{GeV}/c$. These LHCb data can be used to tune the AMPT model.

VII. SUMMARY

This paper presents the first measurements of flow harmonic coefficients of charged hadrons as a function of transverse momentum in the forward direction using PbPb collision data at center-of-mass energy of 5.02 TeV. A two-particle angular correlation analysis is used to construct the two-dimensional, $C(\Delta\eta, \Delta\phi)$, and one-dimensional, $C(\Delta\phi)$, correlation functions. The two-dimensional correlations in PbPb show pronounced near- and away-side ridges compared to the published LHCb pPb and Pbp results [44], indicating stronger forward particle flow in PbPb events than in pPb and Pbp events. The one-dimensional azimuthal correlation functions are used to extract the second- and third-order harmonic coefficients, v_2 and v_3, as a function of p_T in various centrality ranges.

These v_2 and v_3 values are generally smaller than those measured by the ALICE and the ATLAS experiments at central pseudorapidity, which could be due to the dominant freeze-out phase in the forward region leading to weaker flow. However, both studies share the same features of rising v_2 and v_3 at $p_T < 2.5\,\text{GeV}/c$, and falling at high p_T. The consistent v_2 and the continuous falling of v_3 at high p_T may be caused by nonflow contributions or limited statistics at high p_T. The AMPT simulations overestimate both v_2 and v_3, suggesting that they require tuning.

These v_2 and v_3 results in the forward direction from LHCb at the TeV energy scale along with other flow measurements at central pseudorapidity will help constrain the theory models of particle flow, and understand the evolution of QGP from the partonic phase to the hadronic phase.

ACKNOWLEDGMENTS

We express our gratitude to our colleagues in the CERN accelerator departments for the excellent performance of the LHC. We thank the technical and administrative staff at the LHCb institutes. We acknowledge support from CERN and from the national agencies: CAPES, CNPq, FAPERJ, and FINEP (Brazil); MOST and NSFC (China); CNRS/IN2P3 (France); BMBF, DFG, and MPG (Germany); INFN (Italy); NWO (Netherlands); MNiSW and NCN (Poland); MCID/IFA (Romania); MICINN (Spain); SNSF and SER (Switzerland); NASU (Ukraine); STFC (United Kingdom); DOE NP and NSF (USA). We acknowledge the computing resources that

TABLE II. Numerical values of the harmonic coefficient $v_2(p_T)$. The lower and upper uncertainties are denoted as σ^- and σ^+, respectively.

Mean p_T (GeV/c)	v_2 ($\times 10^2$)	Statistical uncertainty ($\times 10^2$)	Systematic uncertainty σ^- ($\times 10^2$)	Systematic uncertainty σ^+ ($\times 10^2$)
Centrality 65–75%				
0.3	1.293	0.027	0.27	0.30
0.5	4.328	0.027	0.23	0.30
0.7	6.885	0.031	0.29	0.34
0.9	9.060	0.038	0.36	0.32
1.2	11.708	0.035	0.094	0.15
1.7	14.232	0.056	0.083	0.21
2.2	15.375	0.090	0.16	0.18
2.7	15.22	0.14	0.19	0.18
3.4	14.33	0.17	0.16	0.16
4.4	13.12	0.34	0.47	0.47
5.7	10.3	0.5	0.4	0.6
8.0	10.3	1.0	1.2	1.1
Centrality 75–84%				
0.3	1.850	0.027	0.60	0.59
0.5	5.187	0.030	0.36	0.36
0.7	7.568	0.036	0.24	0.26
0.9	9.459	0.045	0.19	0.18
1.2	11.582	0.042	0.22	0.23
1.7	13.994	0.069	0.33	0.24
2.2	14.96	0.11	0.33	0.20
2.7	15.22	0.17	0.38	0.32
3.4	15.15	0.21	0.49	0.24
4.4	14.9	0.4	0.5	0.6
5.7	15.36	0.60	1.2	1.2
8.0	16.1	1.2	2.8	2.8

TABLE III. Numerical values of the harmonic coefficient $v_3(p_T)$. The lower and upper uncertainties are denoted as σ^- and σ^+, respectively.

Mean p_T (GeV/c)	v_3 ($\times 10^2$)	Statistical uncertainty ($\times 10^2$)	Systematic uncertainty σ^- ($\times 10^2$)	Systematic uncertainty σ^+ ($\times 10^2$)
Centrality 65–75%				
0.3	−0.31	0.10	0.23	0.22
0.5	1.01	0.10	0.21	0.11
0.7	2.12	0.12	0.21	0.21
0.9	2.49	0.14	0.20	0.08
1.2	3.34	0.13	0.17	0.17
1.7	4.63	0.22	0.36	0.36
2.2	5.00	0.35	0.48	0.48
2.7	4.6	0.5	0.7	0.4
3.4	2.73	0.66	0.30	0.60
4.4	2.72	1.3	0.77	0.45
5.7	−1.3	1.9	2.7	2.7
8.0	−5.6	3.8	1.5	1.5
Centrality 75–84%				
0.3	−0.90	0.14	0.26	0.30
0.5	1.13	0.15	0.28	0.28
0.7	2.14	0.19	0.24	0.12
0.9	2.20	0.23	0.28	0.28
1.2	3.32	0.22	0.16	0.15
1.7	4.15	0.36	0.24	0.20
2.2	3.10	0.56	1.3	1.3
2.7	3.0	0.9	0.6	0.6
3.4	1.67	1.1	0.74	1.2
4.4	−1.0	2.1	2.2	1.6
5.7	−8.7	3.0	2.6	3.2
8.0	−14	6	8	9

are provided by CERN, IN2P3 (France), KIT and DESY (Germany), INFN (Italy), SURF (Netherlands), PIC (Spain), GridPP (United Kingdom), CSCS (Switzerland), IFIN-HH (Romania), CBPF (Brazil), and Polish WLCG (Poland). We are indebted to the communities behind the multiple open-source software packages on which we depend. Individual groups or members have received support from ARC and ARDC (Australia); Key Research Program of Frontier Sciences of CAS, CAS PIFI, CAS CCEPP, Fundamental Research Funds for the Central Universities, and Sci. & Tech. Program of Guangzhou (China); Minciencias (Colombia); EPLANET, Marie Skłodowska-Curie Actions, ERC and NextGenerationEU (European Union); A*MIDEX, ANR, IPhU and Labex P2IO, and Région Auvergne-Rhône-Alpes (France); AvH Foundation (Germany); ICSC (Italy); GVA, XuntaGal, GENCAT, Inditex, InTalent, and Prog. Atracción Talento, CM (Spain); SRC (Sweden); the Leverhulme Trust, the Royal Society, and UKRI (United Kingdom).

APPENDIX: NUMERICAL RESULTS

See Tables II and III for the numerical values of the harmonic coefficients v_2 and v_3.

[1] K. Adcox *et al.* (PHENIX Collaboration), Formation of dense partonic matter in relativistic nucleus-nucleus collisions at RHIC: Experimental evaluation by the PHENIX Collaboration, Nucl. Phys. A **757**, 184 (2005).

[2] O. K. Kalashnikov and V. V. Klimov, Phase transition in the quark-gluon plasma, Phys. Lett. B **88**, 328 (1979).

[3] J. Adams *et al.* (STAR collaboration), Experimental and theoretical challenges in the search for the quark gluon plasma: The STAR Collaboration's critical assessment of the evidence from RHIC collisions, Nucl. Phys. A **757**, 102 (2005).

[4] B. B. Back *et al.* (PHOBOS Collaboration), The PHOBOS perspective on discoveries at RHIC, Nucl. Phys. A **757**, 28 (2005).

[5] I. Arsene *et al.* (BRAHMS Collaboration), Quark gluon plasma and color glass condensate at RHIC? The perspective from the BRAHMS experiment, Nucl. Phys. A **757**, 1 (2005).

[6] P. K. Kovtun, D. T. Son, and A. O. Starinets, Viscosity in strongly interacting quantum field theories from black hole physics, Phys. Rev. Lett. **94**, 111601 (2005).

[7] H. Song, S. A. Bass, and U. Heinz, Elliptic flow in $\sqrt{s} = 200$ GeV Au+Au collisions and $\sqrt{s} = 2.76$ TeV Pb+Pb collisions: Insights from viscous hydrodynamics+hadron cascade hybrid model, Phys. Rev. C **83**, 054912 (2011).

[8] E. Molnár, H. Holopainen, P. Huovinen, and H. Niemi, Influence of temperature-dependent shear viscosity on elliptic flow at backward and forward rapidities in ultrarelativistic heavy-ion collisions, Phys. Rev. C **90**, 044904 (2014).

[9] G. Denicol, A. Monnai, and B. Schenke, Moving forward to constrain the shear viscosity of QCD matter, Phys. Rev. Lett. **116**, 212301 (2016).

[10] C. Aidala *et al.* (PHENIX Collaboration), Creation of quark-gluon plasma droplets with three distinct geometries, Nat. Phys. **15**, 214 (2019).

[11] J. Adam *et al.* (STAR Collaboration), Azimuthal harmonics in small and large collision systems at RHIC top energies, Phys. Rev. Lett. **122**, 172301 (2019).

[12] S. Chatrchyan *et al.* (CMS Collaboration), Multiplicity and transverse momentum dependence of two- and four-particle correlations in pPb and PbPb collisions, Phys. Lett. B **724**, 213 (2013).

[13] G. Aad *et al.* (ATLAS Collaboration), Measurement of the azimuthal anisotropy of charged-particle production in Xe + Xe collisions at $\sqrt{s_{NN}} = 5.44$ TeV with the ATLAS detector, Phys. Rev. C **101**, 024906 (2020).

[14] B. Abelev *et al.* (ALICE Collaboration), Anisotropic flow of charged hadrons, pions and (anti-)protons measured at high transverse momentum in Pb-Pb collisions at $\sqrt{s_{NN}} = 2.76$ TeV, Phys. Lett. B **719**, 18 (2013).

[15] S. Acharya *et al.* (ALICE Collaboration), Anisotropic flow and flow fluctuations of identified hadrons in Pb-Pb collisions at $\sqrt{s_{NN}} = 5.02$ TeV, J. High Energy Phys. 05 (2023) 243.

[16] M. S. Abdallah *et al.* (STAR Collaboration), Flow and interferometry results from Au + Au collisions at $\sqrt{s_{NN}} = 4.5$ GeV, Phys. Rev. C **103**, 034908 (2021).

[17] L. Adamczyk *et al.* (STAR Collaboration), Measurement of elliptic flow of light nuclei at $\sqrt{s_{NN}} = 200$, 62.4, 39, 27, 19.6, 11.5, and 7.7 GeV at the BNL Relativistic Heavy Ion Collider, Phys. Rev. C **94**, 034908 (2016).

[18] S. Acharya *et al.* (ALICE Collaboration), Energy dependence and fluctuations of anisotropic flow in Pb-Pb collisions at $\sqrt{s_{\rm NN}} = 5.02$ and 2.76 TeV, J. High Energy Phys. 07 (2018) 103.

[19] G. Aad *et al.* (ATLAS Collaboration), Two-particle azimuthal correlations in photonuclear ultraperipheral Pb+Pb collisions at 5.02 TeV with ATLAS, Phys. Rev. C **104**, 014903 (2021).

[20] B. B. Back *et al.* (PHOBOS Collaboration), Pseudorapidity and centrality dependence of the collective flow of charged particles in Au+Au collisions at $\sqrt{s_{NN}} = 130$ GeV, Phys. Rev. Lett. **89**, 222301 (2002).

[21] B. B. Back *et al.* (PHOBOS Collaboration), Energy dependence of directed flow over a wide range of pseudorapidity in Au+Au collisions at the BNL Relativistic Heavy Ion Collider, Phys. Rev. Lett. **97**, 012301 (2006).

[22] J. Adam *et al.* (ALICE Collaboration), Pseudorapidity dependence of the anisotropic flow of charged particles in Pb+Pb collisions at $\sqrt{s_{NN}} = 2.76$ TeV, Phys. Lett. B **762**, 376 (2016).

[23] S. Acharya *et al.* (ALICE Collaboration), Search for collectivity with azimuthal J/ψ-hadron correlations in high multiplicity p-Pb collisions at $\sqrt{s_{\rm NN}} = 5.02$ and 8.16 TeV, Phys. Lett. B **780**, 7 (2018).

[24] S. Acharya *et al.* (ALICE Collaboration), J/ψ elliptic flow in Pb-Pb collisions at $\sqrt{s_{NN}} = 5.02$ TeV, Phys. Rev. Lett. **119**, 242301 (2017).

[25] M. Aaboud *et al.* (ATLAS Collaboration), Measurement of the azimuthal anisotropy of charged particles produced in $\sqrt{s_{\rm NN}} = 5.02$ TeV Pb+Pb collisions with the ATLAS detector, Eur. Phys. J. C **78**, 997 (2018).

[26] J. Adam *et al.* (ALICE Collaboration), Forward-central two-particle correlations in p-Pb collisions at $\sqrt{s_{NN}} = 5.02$ TeV, Phys. Lett. B **753**, 126 (2016).

[27] R. Aaij *et al.* (LHCb Collaboration), Centrality determination in heavy-ion collisions with the LHCb detector, J. Instrum. **17**, P05009 (2022).

[28] Z.-W. Lin, C. M. Ko, B.-A. Li, B. Zhang, and S. Pal, Multiphase transport model for relativistic heavy ion collisions, Phys. Rev. C **72**, 064901 (2005).

[29] Z.-W. Lin and L. Zheng, Further developments of a multi-phase transport model for relativistic nuclear collisions, Nucl. Sci. Tech. **32**, 113 (2021).

[30] A. A. Alves, Jr. *et al.* (The LHCb Collaboration), The LHCb detector at the LHC, J. Instrum. **3**, S08005 (2008).

[31] R. Aaij *et al.* (The LHCb Collaboration), LHCb detector performance, Int. J. Mod. Phys. A **30**, 1530022 (2015).

[32] R. Aaij *et al.*, Performance of the LHCb Vertex Locator, J. Instrum. **9**, P09007 (2014).

[33] R. Arink *et al.*, Performance of the LHCb outer tracker, J. Instrum. **9**, P01002 (2014).

[34] P. d'Argent *et al.*, Improved performance of the LHCb Outer Tracker in LHC Run 2, J. Instrum. **12**, P11016 (2017).

[35] R. Aaij *et al.*, The LHCb trigger and its performance in 2011, J. Instrum. **8**, P04022 (2013).

[36] T. Pierog, Iu. Karpenko, J. M. Katzy, E. Yatsenko, and K. Werner, EPOS LHC: Test of collective hadronization with data measured at the CERN Large Hadron Collider, Phys. Rev. C **92**, 034906 (2015).

[37] I. Belyaev *et al.* (The LHCb Collaboration), Handling of the generation of primary events in Gauss, the LHCb simulation framework, J. Phys.: Conf. Ser. **331**, 032047 (2011).

[38] D. J. Lange, The EvtGen particle decay simulation package, Nucl. Instrum. Methods Phys. Res. Sect. A **462**, 152 (2001).

[39] N. Davidson, T. Przedzinski, and Z. Was, PHOTOS interface in C++: Technical and physics documentation, Comput. Phys. Commun. **199**, 86 (2016).

[40] J. Allison *et al.* (Geant4 Collaboration), Geant4 developments and applications, IEEE Trans. Nucl. Sci. **53**, 270 (2006); S. Agostinelli *et al.* (Geant4 Collaboration), Geant4: A simulation toolkit, Nucl. Instrum. Methods Phys. Res. Sect. A **506**, 250 (2003).

[41] M. Clemencic *et al.* (The LHCb Collaboration), LHCb Simulation application, Gauss: Design, evolution and experience, J. Phys.: Conf. Ser. **331**, 032023 (2011).

[42] N. Borghini, P. M. Dinh, and J. Y. Ollitrault, Flow analysis from multiparticle azimuthal correlations, Phys. Rev. C **64**, 054901 (2001).

[43] R. Aaij *et al.* (LHCb Collaboration), Measurement of the nuclear modification factor and prompt charged particle production in *p*Pb and *pp* collisions at $\sqrt{s_{NN}} = 5$ TeV, Phys. Rev. Lett. **128**, 142004 (2022).

[44] R. Aaij *et al.* (LHCb Collaboration), Measurements of long-range near-side angular correlations in $\sqrt{s_{NN}} = 5$ TeV

proton-lead collisions in the forward region, Phys. Lett. B **762**, 473 (2016).

[45] G. Aad *et al.* (ATLAS Collaboration), Measurement of long-range pseudorapidity correlations and azimuthal harmonics in $\sqrt{s_{NN}} = 5.02$ TeV proton-lead collisions with the ATLAS detector, Phys. Rev. C **90**, 044906 (2014).

[46] O. Callot and S. Hansmann-Menzemer, The forward tracking: algorithm and performance studies, CERN Report No. LHCb-2007-015, 2007, https://cds.cern.ch/record/1033584.

[47] K. Aamodt *et al.* (ALICE Collaboration), Harmonic decomposition of two particle angular correlations in Pb-Pb collisions at $\sqrt{s_{NN}} = 2.76$ TeV, Phys. Lett. B **708**, 249 (2012).

R. Aaij,[35] A. S. W. Abdelmotteleb,[54] C. Abellan Beteta,[48] F. Abudinén,[54] T. Ackernley,[58] B. Adeva,[44] M. Adinolfi,[52] P. Adlarson,[78] C. Agapopoulou,[46] C. A. Aidala,[79] Z. Ajaltouni,[11] S. Akar,[63] K. Akiba,[35] P. Albicocco,[25] J. Albrecht,[17] F. Alessio,[46] M. Alexander,[57] A. Alfonso Albero,[43] Z. Aliouche,[60] P. Alvarez Cartelle,[53] R. Amalric,[15] S. Amato,[3] J. L. Amey,[52] Y. Amhis,[13,46] L. An,[6] L. Anderlini,[24] M. Andersson,[48] A. Andreianov,[41] P. Andreola,[48] M. Andreotti,[23] D. Andreou,[66] A. A. Anelli,[28] D. Ao,[7] F. Archilli,[34,a] M. Argenton,[23] S. Arguedas Cuendis,[9] A. Artamonov,[41] M. Artuso,[66] E. Aslanides,[12] M. Atzeni,[62] B. Audurier,[14] D. Bacher,[61] I. Bachiller Perea,[10] S. Bachmann,[19] M. Bachmayer,[47] J. J. Back,[54] A. Bailly-reyre,[15] P. Baladron Rodriguez,[44] V. Balagura,[14] W. Baldini,[23] J. Baptista de Souza Leite,[2] M. Barbetti,[24,b] I. R. Barbosa,[67] R. J. Barlow,[60] S. Barsuk,[13] W. Barter,[56] M. Bartolini,[53] F. Baryshnikov,[41] J. M. Basels,[16] G. Bassi,[32,c] B. Batsukh,[5] A. Battig,[17] A. Bay,[47] A. Beck,[54] M. Becker,[17] F. Bedeschi,[32] I. B. Bediaga,[2] A. Beiter,[66] S. Belin,[44] V. Bellee,[48] K. Belous,[41] I. Belov,[26] I. Belyaev,[41] G. Benane,[12] G. Bencivenni,[25] E. Ben-Haim,[15] A. Berezhnoy,[41] R. Bernet,[48] S. Bernet Andres,[42] H. C. Bernstein,[66] C. Bertella,[60] A. Bertolin,[30] C. Betancourt,[48] F. Betti,[56] J. Bex,[53] Ia. Bezshyiko,[48] J. Bhom,[38] M. S. Bieker,[17] N. V. Biesuz,[23] P. Billoir,[15] A. Biolchini,[35] M. Birch,[59] F. C. R. Bishop,[10] A. Bitadze,[60] A. Bizzeti, M. P. Blago,[53] T. Blake,[54] F. Blanc,[47] J. E. Blank,[17] S. Blusk,[66] D. Bobulska,[57] V. Bocharnikov,[41] J. A. Boelhauve,[17] O. Boente Garcia,[14] T. Boettcher,[63] A. Bohare,[56] A. Boldyrev,[41] C. S. Bolognani,[76] R. Bolzonella,[23,d] N. Bondar,[41] F. Borgato,[30,46] S. Borghi,[60] M. Borsato,[28] J. T. Borsuk,[38] S. A. Bouchiba,[47] T. J. V. Bowcock,[58] A. Boyer,[46] C. Bozzi,[23] M. J. Bradley,[59] S. Braun,[64] A. Brea Rodriguez,[44] N. Breer,[17] J. Brodzicka,[38] A. Brossa Gonzalo,[44] J. Brown,[58] D. Brundu,[29] A. Buonaura,[48] L. Buonincontri,[30] A. T. Burke,[60] C. Burr,[46] A. Bursche,[69] A. Butkevich,[41] J. S. Butter,[53] J. Buytaert,[46] W. Byczynski,[46] S. Cadeddu,[29] H. Cai,[71] R. Calabrese,[23,d] L. Calefice,[17] S. Cali,[25] M. Calvi,[28,e] M. Calvo Gomez,[42] J. Cambon Bouzas,[44] P. Campana,[25] D. H. Campora Perez,[76] A. F. Campoverde Quezada,[7] S. Capelli,[28,e] L. Capriotti,[23] R. C. Caravaca Mora,[9] A. Carbone,[22,f] L. Carcedo Salgado,[44] R. Cardinale,[26,g] A. Cardini,[29] P. Carniti,[28,e] L. Carus,[19] A. Casais Vidal,[62] R. Caspary,[19] G. Casse,[58] J. Castro Godinez,[9] M. Cattaneo,[46] G. Cavallero,[23] V. Cavallini,[23,d] S. Celani,[47] J. Cerasoli,[12] D. Cervenkov,[61] S. Cesare,[27,h] A. J. Chadwick,[58] I. Chahrour,[79] M. Charles,[15] Ph. Charpentier,[46] C. A. Chavez Barajas,[58] M. Chefdeville,[10] C. Chen,[12] S. Chen,[5] A. Chernov,[38] S. Chernyshenko,[50] V. Chobanova,[44,i] S. Cholak,[47] M. Chrzaszcz,[38] A. Chubykin,[41] V. Chulikov,[41] P. Ciambrone,[25] M. F. Cicala,[54] X. Cid Vidal,[44] G. Ciezarek,[46] P. Cifra,[46] P. E. L. Clarke,[56] M. Clemencic,[46] H. V. Cliff,[53] J. Closier,[46] J. L. Cobbledick,[60] C. Cocha Toapaxi,[19] V. Coco,[46] J. Cogan,[12] E. Cogneras,[11] L. Cojocariu,[40] P. Collins,[46] T. Colombo,[46] A. Comerma-Montells,[43] L. Congedo,[21] A. Contu,[29] N. Cooke,[57] I. Corredoira,[44] A. Correia,[15] G. Corti,[46] J. J. Cottee Meldrum,[52] B. Couturier,[46] D. C. Craik,[48] M. Cruz Torres,[2,j] R. Currie,[56] C. L. Da Silva,[65] S. Dadabaev,[41] L. Dai,[68] X. Dai,[6] E. Dall'Occo,[17] J. Dalseno,[44] C. D'Ambrosio,[46] J. Daniel,[11] A. Danilina,[41] P. d'Argent,[21] A. Davidson,[54] J. E. Davies,[60] A. Davis,[60] O. De Aguiar Francisco,[60] C. De Angelis,[29,k] J. de Boer,[35] K. De Bruyn,[75] S. De Capua,[60] M. De Cian,[19,46] U. De Freitas Carneiro Da Graca,[2,l] E. De Lucia,[25] J. M. De Miranda,[2] L. De Paula,[3] M. De Serio,[21,m] D. De Simone,[48] P. De Simone,[25] F. De Vellis,[17] J. A. de Vries,[76] F. Debernardis,[21,m] D. Decamp,[10] V. Dedu,[12] L. Del Buono,[15] B. Delaney,[62] H.-P. Dembinski,[17] J. Deng,[8] V. Denysenko,[48] O. Deschamps,[11] F. Dettori,[29,k] B. Dey,[74] P. Di Nezza,[25] I. Diachkov,[41] S. Didenko,[41] S. Ding,[66] V. Dobishuk,[50] A. D. Docheva,[57] A. Dolmatov,[41] C. Dong,[4] A. M. Donohoe,[20] F. Dordei,[29] A. C. dos Reis,[2] L. Douglas,[57] A. G. Downes,[10] W. Duan,[69] P. Duda,[77] M. W. Dudek,[38] L. Dufour,[46] V. Duk,[31] P. Durante,[46] M. M. Duras,[77] J. M. Durham,[65] A. Dziurda,[38] A. Dzyuba,[41] S. Easo,[55,46] E. Eckstein,[73] U. Egede,[1] A. Egorychev,[41] V. Egorychev,[41] C. Eirea Orro,[44] S. Eisenhardt,[56] E. Ejopu,[60] S. Ek-In,[47] L. Eklund,[78] M. Elashri,[63] J. Ellbracht,[17] S. Ely,[59] A. Ene,[40] E. Epple,[63] S. Escher,[16] J. Eschle,[48] S. Esen,[48] T. Evans,[60] F. Fabiano,[29,46,k] L. N. Falcao,[2] Y. Fan,[7] B. Fang,[71,13] L. Fantini,[31,n] M. Faria,[47] K. Farmer,[56] D. Fazzini,[28,e] L. Felkowski,[77] M. Feng,[5,7] M. Feo,[46] M. Fernandez Gomez,[44] A. D. Fernez,[64] F. Ferrari,[22] F. Ferreira Rodrigues,[3] S. Ferreres Sole,[35] M. Ferrillo,[48] M. Ferro-Luzzi,[46] S. Filippov,[41] R. A. Fini,[21] M. Fiorini,[23,d] M. Firlej,[37] K. M. Fischer,[61] D. S. Fitzgerald,[79] C. Fitzpatrick,[60] T. Fiutowski,[37] F. Fleuret,[14] M. Fontana,[22] F. Fontanelli,[26,g] L. F. Foreman,[60] R. Forty,[46] D. Foulds-Holt,[53] M. Franco Sevilla,[64] M. Frank,[46] E. Franzoso,[23,d] G. Frau,[19] C. Frei,[46] D. A. Friday,[60] L. Frontini,[27,h] J. Fu,[7] Q. Fuehring,[17] Y. Fujii,[1]

T. Fulghesu,[15] E. Gabriel,[35] G. Galati,[21,m] M. D. Galati,[35] A. Gallas Torreira,[44] D. Galli,[22,f] S. Gambetta,[56,46] M. Gandelman,[3] P. Gandini,[27] H. Gao,[7] R. Gao,[61] Y. Gao,[8] Y. Gao,[6] Y. Gao,[8] M. Garau,[29,k] L. M. Garcia Martin,[47] P. Garcia Moreno,[43] J. García Pardiñas,[46] B. Garcia Plana,[44] K. G. Garg,[8] L. Garrido,[43] C. Gaspar,[46] R. E. Geertsema,[35] L. L. Gerken,[17] E. Gersabeck,[60] M. Gersabeck,[60] T. Gershon,[54] Z. Ghorbanimoghaddam,[52] L. Giambastiani,[30] F. I. Giasemis,[15,o] V. Gibson,[53] H. K. Giemza,[39] A. L. Gilman,[61] M. Giovannetti,[25] A. Gioventù,[43] P. Gironella Gironell,[43] C. Giugliano,[23,d] M. A. Giza,[38] E. L. Gkougkousis,[59] F. C. Glaser,[13,19] V. V. Gligorov,[15] C. Göbel,[67] E. Golobardes,[42] D. Golubkov,[41] A. Golutvin,[59,41,46] A. Gomes,[2,p,q] S. Gomez Fernandez,[43] F. Goncalves Abrantes,[61] M. Goncerz,[38] G. Gong,[4] J. A. Gooding,[17] I. V. Gorelov,[41] C. Gotti,[28] J. P. Grabowski,[73] L. A. Granado Cardoso,[46] E. Graugés,[43] E. Graverini,[47] L. Grazette,[54] G. Graziani, A. T. Grecu,[40] L. M. Greeven,[35] N. A. Grieser,[63] L. Grillo,[57] S. Gromov,[41] C. Gu,[14] M. Guarise,[23] M. Guittiere,[13] V. Guliaeva,[41] P. A. Günther,[19] A.-K. Guseinov,[41] E. Gushchin,[41] Y. Guz,[6,41,46] T. Gys,[46] T. Hadavizadeh,[1] C. Hadjivasiliou,[64] G. Haefeli,[47] C. Haen,[46] J. Haimberger,[46] M. Hajheidari,[46] T. Halewood-leagas,[58] M. M. Halvorsen,[46] P. M. Hamilton,[64] J. Hammerich,[58] Q. Han,[8] X. Han,[19] S. Hansmann-Menzemer,[19] L. Hao,[7] N. Harnew,[61] T. Harrison,[58] M. Hartmann,[13] C. Hasse,[46] J. He,[7,r] K. Heijhoff,[35] F. Hemmer,[46] C. Henderson,[63] R. D. L. Henderson,[1,54] A. M. Hennequin,[46] K. Hennessy,[58] L. Henry,[47] J. Herd,[59] P. Herrero Gascon,[19] J. Heuel,[16] A. Hicheur,[3] D. Hill,[47] S. E. Hollitt,[17] J. Horswill,[60] R. Hou,[8] Y. Hou,[10] N. Howarth,[58] J. Hu,[19] J. Hu,[69] W. Hu,[6] X. Hu,[4] W. Huang,[7] W. Hulsbergen,[35] R. J. Hunter,[54] M. Hushchyn,[41] D. Hutchcroft,[58] M. Idzik,[37] D. Ilin,[41] P. Ilten,[63] A. Inglessi,[41] A. Iniukhin,[41] A. Ishteev,[41] K. Ivshin,[41] R. Jacobsson,[46] H. Jage,[16] S. J. Jaimes Elles,[45,72] S. Jakobsen,[46] E. Jans,[35] B. K. Jashal,[45] A. Jawahery,[64] V. Jevtic,[17] E. Jiang,[64] X. Jiang,[5,7] Y. Jiang,[7] Y. J. Jiang,[6] M. John,[61] D. Johnson,[51] C. R. Jones,[53] T. P. Jones,[54] S. Joshi,[39] B. Jost,[46] N. Jurik,[46] I. Juszczak,[38] D. Kaminaris,[47] S. Kandybei,[49] Y. Kang,[4] M. Karacson,[46] D. Karpenkov,[41] M. Karpov,[41] A. M. Kauniskangas,[47] J. W. Kautz,[63] F. Keizer,[46] D. M. Keller,[66] M. Kenzie,[53] T. Ketel,[35] B. Khanji,[66] A. Kharisova,[41] S. Kholodenko,[32] G. Khreich,[13] T. Kirn,[16] V. S. Kirsebom,[47] O. Kitouni,[62] S. Klaver,[36] N. Kleijne,[32,c] K. Klimaszewski,[39] M. R. Kmiec,[39] S. Koliiev,[50] L. Kolk,[17] A. Konoplyannikov,[41] P. Kopciewicz,[37,46] P. Koppenburg,[35] M. Korolev,[41] I. Kostiuk,[35] O. Kot,[50] S. Kotriakhova, A. Kozachuk,[41] P. Kravchenko,[41] L. Kravchuk,[41] M. Kreps,[54] S. Kretzschmar,[16] P. Krokovny,[41] W. Krupa,[66] W. Krzemien,[39] J. Kubat,[19] S. Kubis,[77] W. Kucewicz,[38] M. Kucharczyk,[38] V. Kudryavtsev,[41] E. Kulikova,[41] A. Kupsc,[78] B. K. Kutsenko,[12] D. Lacarrere,[46] A. Lai,[29] A. Lampis,[29] D. Lancierini,[48] C. Landesa Gomez,[44] J. J. Lane,[1] R. Lane,[52] C. Langenbruch,[19] J. Langer,[17] O. Lantwin,[41] T. Latham,[54] F. Lazzari,[32,s] C. Lazzeroni,[51] R. Le Gac,[12] S. H. Lee,[79] R. Lefèvre,[11] A. Leflat,[41] S. Legotin,[41] M. Lehuraux,[54] O. Leroy,[12] T. Lesiak,[38] B. Leverington,[19] A. Li,[4] H. Li,[69] K. Li,[8] L. Li,[60] P. Li,[46] P.-R. Li,[70] S. Li,[8] T. Li,[5] T. Li,[69] Y. Li,[8] Y. Li,[5] Z. Li,[66] Z. Lian,[4] X. Liang,[66] C. Lin,[7] T. Lin,[55] R. Lindner,[46] V. Lisovskyi,[47] R. Litvinov,[29,k] G. Liu,[69] H. Liu,[7] K. Liu,[70] Q. Liu,[7] S. Liu,[5,7] Y. Liu,[56] Y. Liu,[70] Y. L. Liu,[59] A. Lobo Salvia,[43] A. Loi,[29] J. Lomba Castro,[44] T. Long,[53] J. H. Lopes,[3] A. Lopez Huertas,[43] S. López Soliño,[44] G. H. Lovell,[53] C. Lucarelli,[24,b] D. Lucchesi,[30,t] S. Luchuk,[41] M. Lucio Martinez,[76] V. Lukashenko,[35,50] Y. Luo,[4] A. Lupato,[30] E. Luppi,[23,d] K. Lynch,[20] X.-R. Lyu,[7] G. M. Ma,[4] R. Ma,[7] S. Maccolini,[17] F. Machefert,[13] F. Maciuc,[40] I. Mackay,[61] L. R. Madhan Mohan,[53] M. M. Madurai,[51] A. Maevskiy,[41] D. Magdalinski,[35] D. Maisuzenko,[41] M. W. Majewski,[37] J. J. Malczewski,[38] S. Malde,[61] B. Malecki,[38,46] L. Malentacca,[46] A. Malinin,[41] T. Maltsev,[41] G. Manca,[29,k] G. Mancinelli,[12] C. Mancuso,[27,13,h] R. Manera Escalero,[43] D. Manuzzi,[22] D. Marangotto,[27,h] J. F. Marchand,[10] R. Marchevski,[47] U. Marconi,[22] S. Mariani,[46] C. Marin Benito,[43,46] J. Marks,[19] A. M. Marshall,[52] P. J. Marshall,[58] G. Martelli,[31,n] G. Martellotti,[33] L. Martinazzoli,[46] M. Martinelli,[28,e] D. Martinez Santos,[44] F. Martinez Vidal,[45] A. Massafferri,[2] M. Materok,[16] R. Matev,[46] A. Mathad,[48] V. Matiunin,[41] C. Matteuzzi,[66] K. R. Mattioli,[14] A. Mauri,[59] E. Maurice,[14] J. Mauricio,[43] P. Mayencourt,[47] M. Mazurek,[46] M. McCann,[59] L. Mcconnell,[20] T. H. McGrath,[60] N. T. McHugh,[57] A. McNab,[60] R. McNulty,[20] B. Meadows,[63] G. Meier,[17] D. Melnychuk,[39] M. Merk,[35,76] A. Merli,[27,h] L. Meyer Garcia,[3] D. Miao,[5,7] H. Miao,[7] M. Mikhasenko,[73,u] D. A. Milanes,[72] A. Minotti,[28,e] E. Minucci,[66] T. Miralles,[11] S. E. Mitchell,[56] B. Mitreska,[17] D. S. Mitzel,[17] A. Modak,[55] A. Mödden,[17] R. A. Mohammed,[61] R. D. Moise,[16] S. Mokhnenko,[41] T. Mombächer,[46] M. Monk,[54,1] I. A. Monroy,[72] S. Monteil,[11] A. Morcillo Gomez,[44] G. Morello,[25] M. J. Morello,[32,c] M. P. Morgenthaler,[19] J. Moron,[37] A. B. Morris,[46] A. G. Morris,[12] R. Mountain,[66] H. Mu,[4] Z. M. Mu,[6] E. Muhammad,[54] F. Muheim,[56] M. Mulder,[75] K. Müller,[48] F. Mũnoz-Rojas,[9] R. Murta,[59] P. Naik,[58] T. Nakada,[47] R. Nandakumar,[55] T. Nanut,[46] I. Nasteva,[3] M. Needham,[56] N. Neri,[27,h] S. Neubert,[73] N. Neufeld,[46] P. Neustroev,[41] R. Newcombe,[59] J. Nicolini,[17,13] D. Nicotra,[76] E. M. Niel,[47] N. Nikitin,[41] P. Nogga,[73] N. S. Nolte,[62] C. Normand,[10,29,k] J. Novoa Fernandez,[44] G. Nowak,[63] C. Nunez,[79] H. N. Nur,[57] A. Oblakowska-Mucha,[37] V. Obraztsov,[41] T. Oeser,[16] S. Okamura,[23,46,d] R. Oldeman,[29,k] F. Oliva,[56] M. Olocco,[17] C. J. G. Onderwater,[76] R. H. O'Neil,[56] J. M. Otalora Goicochea,[3] T. Ovsiannikova,[41] P. Owen,[48] A. Oyanguren,[45] O. Ozcelik,[56] K. O. Padeken,[73] B. Pagare,[54] P. R. Pais,[19] T. Pajero,[61] A. Palano,[21] M. Palutan,[25] G. Panshin,[41] L. Paolucci,[54] A. Papanestis,[55] M. Pappagallo,[21,m] L. L. Pappalardo,[23,d] C. Pappenheimer,[63] C. Parkes,[60] B. Passalacqua,[23,d]

G. Passaleva,[24] D. Passaro,[32] A. Pastore,[21] M. Patel,[59] J. Patoc,[61] C. Patrignani,[22,f] C. J. Pawley,[76] A. Pellegrino,[35] M. Pepe Altarelli,[25] S. Perazzini,[22] D. Pereima,[41] A. Pereiro Castro,[44] P. Perret,[11] A. Perro,[46] K. Petridis,[52] A. Petrolini,[26,g] S. Petrucci,[56] H. Pham,[66] L. Pica,[32] M. Piccini,[31] B. Pietrzyk,[10] G. Pietrzyk,[13] D. Pinci,[33] F. Pisani,[46] M. Pizzichemi,[28,e] V. Placinta,[40] M. Plo Casasus,[44] F. Polci,[15,46] M. Poli Lener,[25] A. Poluektov,[12] N. Polukhina,[41] I. Polyakov,[46] E. Polycarpo,[3] S. Ponce,[46] D. Popov,[7] S. Poslavskii,[41] K. Prasanth,[38] C. Prouve,[44] V. Pugatch,[50] V. Puill,[13] G. Punzi,[32,s] H. R. Qi,[4] W. Qian,[7] N. Qin,[4] S. Qu,[4] R. Quagliani,[47] R. I. Rabadan Trejo,[54] B. Rachwal,[37] J. H. Rademacker,[52] M. Rama,[32] M. Ramírez García,[79] M. Ramos Pernas,[54] M. S. Rangel,[3] F. Ratnikov,[41] G. Raven,[36] M. Rebollo De Miguel,[45] F. Redi,[46] J. Reich,[52] F. Reiss,[60] Z. Ren,[7] P. K. Resmi,[61] R. Ribatti,[32,c] G. R. Ricart,[14,80] D. Riccardi,[32] S. Ricciardi,[55] K. Richardson,[62] M. Richardson-Slipper,[56] K. Rinnert,[58] P. Robbe,[13] G. Robertson,[57] E. Rodrigues,[58,46] E. Rodriguez Fernandez,[44] J. A. Rodriguez Lopez,[72] E. Rodriguez Rodriguez,[44] A. Rogovskiy,[55] D. L. Rolf,[46] A. Rollings,[61] P. Roloff,[46] V. Romanovskiy,[41] M. Romero Lamas,[44] A. Romero Vidal,[44] G. Romolini,[23] F. Ronchetti,[47] M. Rotondo,[25] S. R. Roy,[19] M. S. Rudolph,[66] T. Ruf,[46] M. Ruiz Diaz,[19] R. A. Ruiz Fernandez,[44] J. Ruiz Vidal,[78,v] A. Ryzhikov,[41] J. Ryzka,[37] J. J. Saborido Silva,[44] R. Sadek,[14] N. Sagidova,[41] N. Sahoo,[51] B. Saitta,[29,k] M. Salomoni,[28,e] C. Sanchez Gras,[35] I. Sanderswood,[45] R. Santacesaria,[33] C. Santamarina Rios,[44] M. Santimaria,[25] L. Santoro,[2] E. Santovetti,[34] A. Saputi,[23,46] D. Saranin,[41] G. Sarpis,[56] M. Sarpis,[73] A. Sarti,[33] C. Satriano,[33,w] A. Satta,[34] M. Saur,[6] D. Savrina,[41] H. Sazak,[11] L. G. Scantlebury Smead,[61] A. Scarabotto,[15] S. Schael,[16] S. Scherl,[58] A. M. Schertz,[74] M. Schiller,[57] H. Schindler,[46] M. Schmelling,[18] B. Schmidt,[46] S. Schmitt,[16] H. Schmitz,[73] O. Schneider,[47] A. Schopper,[46] N. Schulte,[17] S. Schulte,[47] M. H. Schune,[13] R. Schwemmer,[46] G. Schwering,[16] B. Sciascia,[25] A. Sciuccati,[46] S. Sellam,[44] A. Semennikov,[41] M. Senghi Soares,[36] A. Sergi,[26,g] N. Serra,[48,46] L. Sestini,[30] A. Seuthe,[17] Y. Shang,[6] D. M. Shangase,[79] M. Shapkin,[41] I. Shchemerov,[41] L. Shchutska,[47] T. Shears,[58] L. Shekhtman,[41] Z. Shen,[6] S. Sheng,[5,7] V. Shevchenko,[41] B. Shi,[7] E. B. Shields,[28,e] Y. Shimizu,[13] E. Shmanin,[41] R. Shorkin,[41] J. D. Shupperd,[66] R. Silva Coutinho,[66] G. Simi,[30] S. Simone,[21,m] N. Skidmore,[60] R. Skuza,[19] T. Skwarnicki,[66] M. W. Slater,[51] J. C. Smallwood,[61] E. Smith,[62] K. Smith,[65] M. Smith,[59] A. Snoch,[35] L. Soares Lavra,[56] M. D. Sokoloff,[63] F. J. P. Soler,[57] A. Solomin,[41,52] A. Solovev,[41] I. Solovyev,[41] R. Song,[1] Y. Song,[47] Y. Song,[4] Y. S. Song,[6] F. L. Souza De Almeida,[66] B. Souza De Paula,[3] E. Spadaro Norella,[27,h] E. Spedicato,[22] J. G. Speer,[17] E. Spiridenkov,[41] P. Spradlin,[57] V. Sriskaran,[46] F. Stagni,[46] M. Stahl,[46] S. Stahl,[46] S. Stanislaus,[61] E. N. Stein,[46] O. Steinkamp,[48] O. Stenyakin,[41] H. Stevens,[17] D. Strekalina,[41] Y. Su,[7] F. Suljik,[61] J. Sun,[29] L. Sun,[71] Y. Sun,[64] P. N. Swallow,[51] K. Swientek,[37] F. Swystun,[54] A. Szabelski,[39] T. Szumlak,[37] M. Szymanski,[46] Y. Tan,[4] S. Taneja,[60] M. D. Tat,[61] A. Terentev,[48] F. Terzuoli,[32,x] F. Teubert,[46] E. Thomas,[46] D. J. D. Thompson,[51] H. Tilquin,[59] V. Tisserand,[11] S. T'Jampens,[10] M. Tobin,[5] L. Tomassetti,[23,d] G. Tonani,[27,h] X. Tong,[6] D. Torres Machado,[2] L. Toscano,[17] D. Y. Tou,[4] C. Trippl,[42] G. Tuci,[19] N. Tuning,[35] L. H. Uecker,[19] A. Ukleja,[37] D. J. Unverzagt,[19] E. Ursov,[41] A. Usachov,[36] A. Ustyuzhanin,[41] U. Uwer,[19] V. Vagnoni,[22] A. Valassi,[46] G. Valenti,[22] N. Valls Canudas,[42] H. Van Hecke,[65] E. van Herwijnen,[59] C. B. Van Hulse,[44,y] R. Van Laak,[47] M. van Veghel,[35] R. Vazquez Gomez,[43] P. Vazquez Regueiro,[44] C. Vázquez Sierra,[44] S. Vecchi,[23] J. J. Velthuis,[52] M. Veltri,[24,z] A. Venkateswaran,[47] M. Vesterinen,[54] D. Vieira,[63] M. Vieites Diaz,[46] X. Vilasis-Cardona,[42] E. Vilella Figueras,[58] A. Villa,[22] P. Vincent,[15] F. C. Volle,[13] D. vom Bruch,[12] V. Vorobyev,[41] N. Voropaev,[41] K. Vos,[76] G. Vouters,[10] C. Vrahas,[56] J. Walsh,[32] E. J. Walton,[1] G. Wan,[6] C. Wang,[19] G. Wang,[8] J. Wang,[6] J. Wang,[5] J. Wang,[4] J. Wang,[71] M. Wang,[27] N. W. Wang,[7] R. Wang,[52] X. Wang,[69] X. W. Wang,[59] Y. Wang,[8] Z. Wang,[13] Z. Wang,[4] Z. Wang,[7] J. A. Ward,[54,1] N. K. Watson,[51] D. Websdale,[59] Y. Wei,[6] B. D. C. Westhenry,[52] D. J. White,[60] M. Whitehead,[57] A. R. Wiederhold,[54] D. Wiedner,[17] G. Wilkinson,[61] M. K. Wilkinson,[63] M. Williams,[62] M. R. J. Williams,[56] R. Williams,[53] F. F. Wilson,[55] W. Wislicki,[39] M. Witek,[38] L. Witola,[19] C. P. Wong,[65] G. Wormser,[13] S. A. Wotton,[53] H. Wu,[66] J. Wu,[8] Y. Wu,[6] K. Wyllie,[46] S. Xian,[69] Z. Xiang,[5] Y. Xie,[8] A. Xu,[32] J. Xu,[7] L. Xu,[4] L. Xu,[4] M. Xu,[54] Z. Xu,[11] Z. Xu,[7] Z. Xu,[5] D. Yang,[4] S. Yang,[7] X. Yang,[6] Y. Yang,[26] Z. Yang,[6] Z. Yang,[64] V. Yeroshenko,[13] H. Yeung,[60] H. Yin,[8] C. Y. Yu,[6] J. Yu,[68] X. Yuan,[5] E. Zaffaroni,[47] M. Zavertyaev,[18] M. Zdybal,[38] M. Zeng,[4] C. Zhang,[6] D. Zhang,[8] J. Zhang,[7] L. Zhang,[4] S. Zhang,[68] S. Zhang,[6] Y. Zhang,[6] Y. Zhang,[61] Y. Z. Zhang,[4] Y. Zhao,[19] A. Zharkova,[41] A. Zhelezov,[19] X. Z. Zheng,[4] Y. Zheng,[7] T. Zhou,[6] X. Zhou,[8] Y. Zhou,[7] V. Zhovkovska,[54] L. Z. Zhu,[7] X. Zhu,[4] X. Zhu,[8] Z. Zhu,[7] V. Zhukov,[16,41] J. Zhuo,[45] Q. Zou,[5,7] D. Zuliani,[30] and G. Zunica[60]

(LHCb Collaboration)

[1]*School of Physics and Astronomy, Monash University, Melbourne, Australia*
[2]*Centro Brasileiro de Pesquisas Físicas (CBPF), Rio de Janeiro, Brazil*
[3]*Universidade Federal do Rio de Janeiro (UFRJ), Rio de Janeiro, Brazil*
[4]*Center for High Energy Physics, Tsinghua University, Beijing, China*
[5]*Institute of High Energy Physics (IHEP), Beijing, China*

[6]*School of Physics State Key Laboratory of Nuclear Physics and Technology, Peking University, Beijing, China*
[7]*University of Chinese Academy of Sciences, Beijing, China*
[8]*Institute of Particle Physics, Central China Normal University, Wuhan, Hubei, China*
[9]*Consejo Nacional de Rectores (CONARE), San Jose, Costa Rica*
[10]*Université Savoie Mont Blanc, CNRS, IN2P3-LAPP, Annecy, France*
[11]*Université Clermont Auvergne, CNRS/IN2P3, LPC, Clermont-Ferrand, France*
[12]*Aix Marseille Univ, CNRS/IN2P3, CPPM, Marseille, France*
[13]*Université Paris-Saclay, CNRS/IN2P3, IJCLab, Orsay, France*
[14]*Laboratoire Leprince-Ringuet, CNRS/IN2P3, Ecole Polytechnique, Institut Polytechnique de Paris, Palaiseau, France*
[15]*LPNHE, Sorbonne Université, Paris Diderot Sorbonne Paris Cité, CNRS/IN2P3, Paris, France*
[16]*I. Physikalisches Institut, RWTH Aachen University, Aachen, Germany*
[17]*Fakultät Physik, Technische Universität Dortmund, Dortmund, Germany*
[18]*Max-Planck-Institut für Kernphysik (MPIK), Heidelberg, Germany*
[19]*Physikalisches Institut, Ruprecht-Karls-Universität Heidelberg, Heidelberg, Germany*
[20]*School of Physics, University College Dublin, Dublin, Ireland*
[21]*INFN Sezione di Bari, Bari, Italy*
[22]*INFN Sezione di Bologna, Bologna, Italy*
[23]*INFN Sezione di Ferrara, Ferrara, Italy*
[24]*INFN Sezione di Firenze, Firenze, Italy*
[25]*INFN Laboratori Nazionali di Frascati, Frascati, Italy*
[26]*INFN Sezione di Genova, Genova, Italy*
[27]*INFN Sezione di Milano, Milano, Italy*
[28]*INFN Sezione di Milano-Bicocca, Milano, Italy*
[29]*INFN Sezione di Cagliari, Monserrato, Italy*
[30]*Università degli Studi di Padova, Università e INFN, Padova, Padova, Italy*
[31]*INFN Sezione di Perugia, Perugia, Italy*
[32]*INFN Sezione di Pisa, Pisa, Italy*
[33]*INFN Sezione di Roma La Sapienza, Roma, Italy*
[34]*INFN Sezione di Roma Tor Vergata, Roma, Italy*
[35]*Nikhef National Institute for Subatomic Physics, Amsterdam, Netherlands*
[36]*Nikhef National Institute for Subatomic Physics and VU University Amsterdam, Amsterdam, Netherlands*
[37]*AGH - University of Science and Technology, Faculty of Physics and Applied Computer Science, Kraków, Poland*
[38]*Henryk Niewodniczanski Institute of Nuclear Physics Polish Academy of Sciences, Kraków, Poland*
[39]*National Center for Nuclear Research (NCBJ), Warsaw, Poland*
[40]*Horia Hulubei National Institute of Physics and Nuclear Engineering, Bucharest-Magurele, Romania*
[41]*Affiliated with an institute covered by a cooperation agreement with CERN*
[42]*DS4DS, La Salle, Universitat Ramon Llull, Barcelona, Spain*
[43]*ICCUB, Universitat de Barcelona, Barcelona, Spain*
[44]*Instituto Galego de Física de Altas Enerxías (IGFAE), Universidade de Santiago de Compostela, Santiago de Compostela, Spain*
[45]*Instituto de Fisica Corpuscular, Centro Mixto Universidad de Valencia - CSIC, Valencia, Spain*
[46]*European Organization for Nuclear Research (CERN), Geneva, Switzerland*
[47]*Institute of Physics, Ecole Polytechnique Fédérale de Lausanne (EPFL), Lausanne, Switzerland*
[48]*Physik-Institut, Universität Zürich, Zürich, Switzerland*
[49]*NSC Kharkiv Institute of Physics and Technology (NSC KIPT), Kharkiv, Ukraine*
[50]*Institute for Nuclear Research of the National Academy of Sciences (KINR), Kyiv, Ukraine*
[51]*University of Birmingham, Birmingham, United Kingdom*
[52]*H. H. Wills Physics Laboratory, University of Bristol, Bristol, United Kingdom*
[53]*Cavendish Laboratory, University of Cambridge, Cambridge, United Kingdom*
[54]*Department of Physics, University of Warwick, Coventry, United Kingdom*
[55]*STFC Rutherford Appleton Laboratory, Didcot, United Kingdom*
[56]*School of Physics and Astronomy, University of Edinburgh, Edinburgh, United Kingdom*
[57]*School of Physics and Astronomy, University of Glasgow, Glasgow, United Kingdom*
[58]*Oliver Lodge Laboratory, University of Liverpool, Liverpool, United Kingdom*
[59]*Imperial College London, London, United Kingdom*
[60]*Department of Physics and Astronomy, University of Manchester, Manchester, United Kingdom*
[61]*Department of Physics, University of Oxford, Oxford, United Kingdom*
[62]*Massachusetts Institute of Technology, Cambridge, Massachusetts, USA*
[63]*University of Cincinnati, Cincinnati, Ohio, USA*
[64]*University of Maryland, College Park, Maryland, USA*

[65]*Los Alamos National Laboratory (LANL), Los Alamos, New Mexico, USA*
[66]*Syracuse University, Syracuse, New York, USA*
[67]*Pontifícia Universidade Católica do Rio de Janeiro (PUC-Rio), Rio de Janeiro, Brazil, associated to*[3]
[68]*Physics and Micro Electronic College, Hunan University, Changsha City, China, associated to*[8]
[69]*Guangdong Provincial Key Laboratory of Nuclear Science, Guangdong-Hong Kong Joint Laboratory of Quantum Matter, Institute of Quantum Matter, South China Normal University, Guangzhou, China, associated to*[4]
[70]*Lanzhou University, Lanzhou, China, associated to*[5]
[71]*School of Physics and Technology, Wuhan University, Wuhan, China, associated to*[4]
[72]*Departamento de Fisica, Universidad Nacional de Colombia, Bogota, Colombia, associated to*[15]
[73]*Helmholtz-Institut für Strahlen und Kernphysik, Universität Bonn, Bonn, Germany, associated to*[19]
[74]*Eotvos Lorand University, Budapest, Hungary, associated to*[46]
[75]*Van Swinderen Institute, University of Groningen, Groningen, Netherlands, associated to*[35]
[76]*Universiteit Maastricht, Maastricht, Netherlands, associated to*[35]
[77]*Tadeusz Kosciuszko Cracow University of Technology, Cracow, Poland, associated to*[38]
[78]*Department of Physics and Astronomy, Uppsala University, Uppsala, Sweden, associated to*[57]
[79]*University of Michigan, Ann Arbor, Michigan USA, associated to*[66]
[80]*Departement de Physique Nucleaire (SPhN), Gif-Sur-Yvette, France*

[a]Università di Roma Tor Vergata, Roma, Italy.
[b]Università di Firenze, Firenze, Italy.
[c]Scuola Normale Superiore, Pisa, Italy.
[d]Università di Ferrara, Ferrara, Italy.
[e]Università di Milano Bicocca, Milano, Italy.
[f]Università di Bologna, Bologna, Italy.
[g]Università di Genova, Genova, Italy.
[h]Università degli Studi di Milano, Milano, Italy.
[i]Universidade da Coruña, Coruña, Spain.
[j]Universidad Nacional Autónoma de Honduras, Tegucigalpa, Honduras.
[k]Università di Cagliari, Cagliari, Italy.
[l]Centro Federal de Educacão Tecnológica Celso Suckow da Fonseca, Rio De Janeiro, Brazil.
[m]Università di Bari, Bari, Italy.
[n]Università di Perugia, Perugia, Italy.
[o]LIP6, Sorbonne Universite, Paris, France.
[p]Universidade de Brasília, Brasília, Brazil.
[q]Deceased.
[r]Hangzhou Institute for Advanced Study, UCAS, Hangzhou, China.
[s]Università di Pisa, Pisa, Italy.
[t]Università di Padova, Padova, Italy.
[u]Excellence Cluster ORIGINS, Munich, Germany.
[y]Division of Particle Physics, Department of Physics, Lund University, Lund, Sweden.
[w]Università della Basilicata, Potenza, Italy.
[x]Università di Siena, Siena, Italy.
[y]Universidad de Alcalá, Alcalá de Henares, Spain.
[z]Università di Urbino, Urbino, Italy.